



Bis-benzimidazolyl diamide copper (II) complexes: Synthesis, crystal structure and oxidation of substituted amino phenols

Gauri Ahuja, Pavan Mathur*

Department of Chemistry, University of Delhi, Delhi-110007, India

ARTICLE INFO

Article history:

Received 8 July 2011

Accepted 16 December 2011

Available online 24 December 2011

Keywords:

Benzimidazole diamides

Copper (II) complexes

Substituted amino phenols

Phenoxazinone synthase

ABSTRACT

A new tetradentate ligand *N,N'*-Bis (1-butyl-benzimidazol-2-yl-methyl)-hexane-1,6-dicarboxamide (b-GBSA) has been utilized to synthesize mononuclear copper (II) complexes with inner sphere anionic ligands like NO_3^- , Br^- and Cl^- . Two of the complexes $[\text{Cu}(\text{L})\text{NO}_3]\text{NO}_3$ (**1**) and $[\text{Cu}(\text{L})\text{Br}]\text{Br}$ (**2**) have been structurally characterized. The geometry of copper (II) in (**1**) is a distorted octahedral with NO_3^- anion acting as a bidentate ligand, while for (**2**) the geometry is found to be a near square pyramidal. The complexes carry out the oxidation of substituted amino phenols in the presence of molecular oxygen. The oxidation gets blocked at the dihydrophenoxazinone stage for 2-amino-5-methyl phenol, and to o-quinone for 2-amino-4-tertiary butyl phenol, quite like the enzyme phenoxazinone synthase.

© 2011 Elsevier B.V. All rights reserved.

Copper metalloproteins with copper ion at the active site and histidine as one of the ligands are involved in a number of important biological functions, such as electron transfer, oxygen transport and substrate oxidation [1–4]. Phenoxazinone synthase is naturally found in the bacterium *Streptomyces* and catalyzes the oxidative coupling of two molecules of aminophenol to form the phenoxazinone chromophore [5]. The enzyme is a type II copper-containing protein and catalyzes the oxidation of a wide variety of aminophenols to phenoxazinones [6]. Later work has shown that the enzyme catalyzed oxidation of substituted amino phenols blocks the formation of phenoxazinone at various intermediate stages [7].

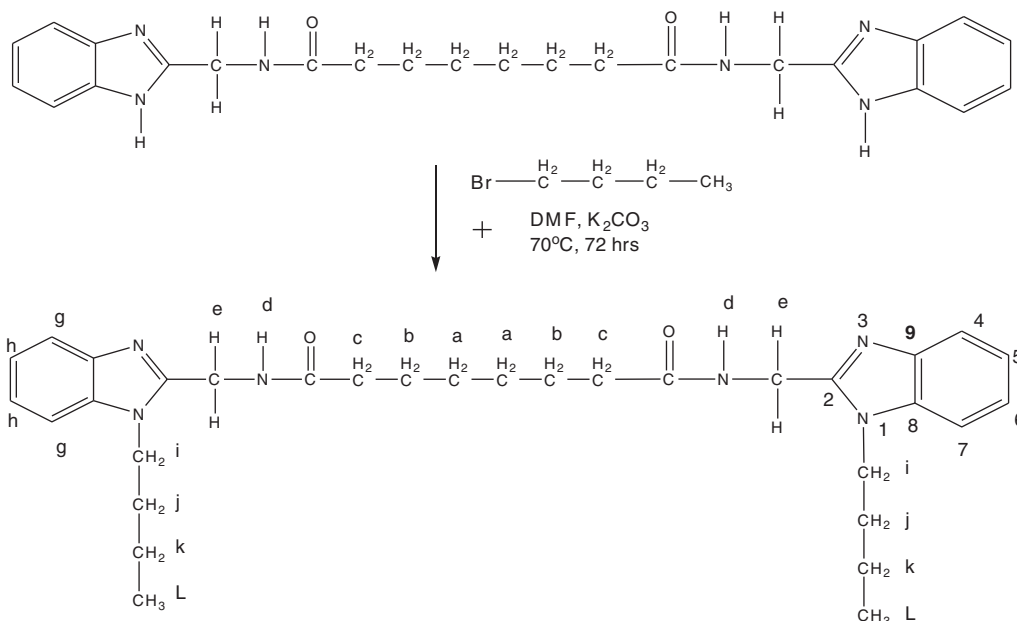
In the present study, a tetradentate bis-benzimidazole di amide ligand *N,N'*-Bis(1-butyl-benzimidazol-2-yl-methyl)-hexane-1,6-dicarboxamide ($\text{L} = \text{b-GBSA}$) (Scheme 1) has been synthesized and characterized [8]. Copper (II) complexes with cupric salts such as $\text{Cu}(\text{NO}_3)_2 \cdot 3\text{H}_2\text{O}$, CuBr_2 and $\text{CuCl}_2 \cdot 2\text{H}_2\text{O}$ with the ligand (L) have been prepared [9]. Two of the copper complexes (**1** and **2**) are characterized by single-crystal X-ray crystallographic measurement [10–13]. The complexes carry out the oxidation of substituted amino phenols to various stages in the presence of molecular oxygen and mimic the phenoxazinone synthase activity.

Spectroscopic grade solvents were used for the spectral and electrochemical studies and the rest were freshly distilled off before use. All other chemicals were obtained from commercial sources and were used as such. Glycine benzimidazole dihydrochloride was prepared following the procedure reported by Cescon and Day [14].

The electronic spectra of the copper (II) complexes were recorded in DMF solution. Two peaks in the range 273–287 nm were observed for all the complexes which have been assigned to intra ligand $\pi-\pi^*$ transition in $-\text{C}=\text{N}-\text{C}=\text{C}-$ system of the benzimidazole moiety. The bands show decreased absorption values in comparison to parent ligand [15]. The copper (II) complexes exhibit a single symmetrical but broad d–d band in the region 690–750 nm, characteristic of copper (II) in a tetragonal geometry [16]. The ligand and its copper (II) complexes have characteristic IR bands in the range 1618–1643 cm^{-1} , 1542–1560 cm^{-1} , and 1451–1465 cm^{-1} . These are assigned to amide I ($\nu_{\text{C}=\text{O}}$ stretching), amide II ($\nu_{\text{C}-\text{N}}$ stretching) and benzimidazole ring ($\nu_{\text{C}=\text{C}-\text{N}=\text{C}}$ stretching). Shifts in the amide band I, due to $\text{C}=\text{O}$ group and in amide II band due to C–N group, is indicative of the coordination of the ligand through the carbonyl oxygen in the complexes [17–19]. The benzene ring gives a peak in the range of 735–745 cm^{-1} . Strong peaks for the nitrate ion is observed at 1384 cm^{-1} (vs) and 823 cm^{-1} (w) in the nitrate complex and are assigned to $\nu_{\text{O}-\text{N}-\text{O}}$ symmetric and antisymmetric stretching frequency [20]. A broad band at 3431 cm^{-1} in the complex (**3**) is assigned to $\nu_{\text{O}-\text{H}}$ stretching, indicating the presence of water of crystallization.

Cyclic voltammograms of the copper (II) complexes were obtained in DMSO: Acetonitrile (8:2) mixed solvent system [Fig. 1.1(a)–(c) Supplementary data] 0.1 M TBAP; Pt vs. Ag/AgNO₃ reference electrode. $E_{1/2}$ values are in the range of –108 mV to –160 mV and are dependent on the coordinated anion. The $E_{1/2}$ follows the order of $\text{NO}_3^- < \text{Cl}^- < \text{Br}^-$. For the present series of copper (II) complexes, $E_{1/2}$ values are not as positive as have been reported for similar benzimidazole diamide complexes [21]. Conductivity measurements were carried out in methanol and molar conductance values were found to be $99.6 \times 10^{-4} \Omega^{-1} \text{cm}^2 \text{mol}^{-1}$, $90.0 \times 10^{-4} \Omega^{-1} \text{cm}^2 \text{mol}^{-1}$ and $79.2 \times 10^{-4} \Omega^{-1} \text{cm}^2 \text{mol}^{-1}$ for complexes (**1**), (**2**) and (**3**)

* Corresponding author. Tel.: +91 1127667725x1381; fax: +91 1127666605.
E-mail address: pavanmat@yahoo.co.in (P. Mathur).



Scheme 1. Synthesis of N,N'-Bis(1-butyl-benzimidazol-2-yl-methyl)-hexane-1,6-dicarboxamide (L = b-GBSA).

respectively. Data shows that they can be regarded as 1:1 electrolytes [22]. EPR spectra of the copper (II) complexes were recorded in DMF at liquid nitrogen temperature [Fig. 2.1(a)–(c) Supplementary data]. The $g > g > 2.0023$ values indicate a $d_{x^2-y^2}$ ground state. For (1) $g = 2.33$, $g = 2.08$, $A = 140$, $g/A * 10^4 = 166$, (2) $g = 2.28$, $g = 2.07$, $A = 140$, $g/A * 10^4 = 162$ (3) $g = 2.35$, $g = 2.06$, $A = 146$, $g/A * 10^4 = 160$. The value of hyperfine splitting constant A is low in comparison to the normal range found for the copper (II) complexes, implying a marked tetrahedral distortion of the equatorial plane [23]. Further no nitrogen super hyperfine splitting could be observed implying non planarity of the complexes. The covalency factor α^2 was found to be in the range of 0.56–0.70 indicating covalent nature of Cu–L bond [24].

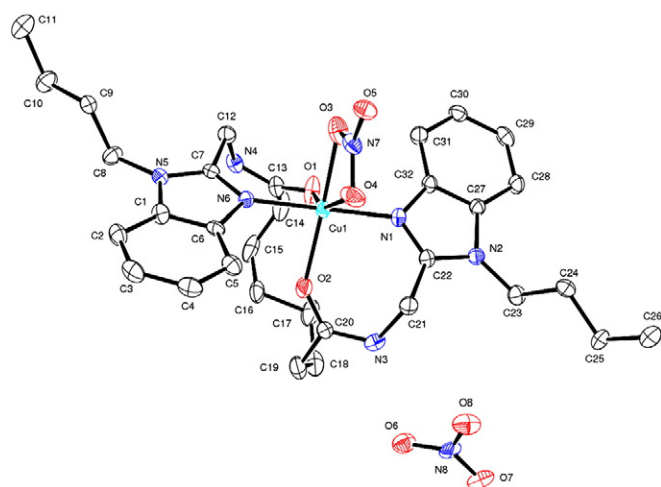


Fig. 1. Ortep diagram of **1** drawn in 30% thermal probability level; hydrogen atoms were omitted for clarity. Selected bond lengths (Å) and bond angles (°): Cu1–O1 2.142(5), Cu1–O2 2.056(5), Cu1–O3 2.140(6), Cu1–O4 2.375(7), Cu1–N1 1.985(5), Cu1–N6 1.971(5), N6–Cu1–N1 178.5(2), N6–Cu1–O2 85.7(2), N1–Cu1–O2 94.9(2), N6–Cu1–O1 95.2(2), N1–Cu1–O1 86.2(2), O2–Cu1–O1 92.7(3), N6–Cu1–O3 88.4(2), N1–Cu1–O3 90.7(2), O2–Cu1–O3 163.6(2), O1–Cu1–O3 103.1(2), N6–Cu1–O4 92.9(2), N1–Cu1–O4 85.6(2), O2–Cu1–O4 108.2(2), O1–Cu1–O4 158.1(2), O3–Cu1–O4 56.84(19).

The copper center in (1) has a tetragonally distorted octahedral environment. The six coordinations comprise of two imine nitrogens of the two benzimidazole rings, two amide carbonyl oxygen atoms and two oxygens of one of the nitrate anions. The carbonyl oxygen atom O2, nitrate oxygen atom O3 and the two benzimidazole nitrogen atoms N1, N6 occupy the equatorial positions of the plane while the axial position is occupied by another amide carbonyl oxygen atom O1 and nitrate oxygen atom O4 to generate distorted octahedral geometry. Bond length shows that nitrate behaves as unsymmetrical bidentate chelating ligand, with Cu1–O4 bond length of 2.375 Å being much longer than Cu1–O3 bond length of 2.140 Å. The bond angle between O3–Cu1–O4 of 56.84°(19) is in the range for weakly coordinating bidentate ligands [20,25] (Fig. 1).

The structure of the above complex is similar in some respects to that found earlier for a copper nitrate complex of a related benzimidazole diamide ligand [20]. The bond distances of 1.985(5) Å Cu–N6 and 1.971(5) Å Cu–N1 are found to be typically similar with other imidazole/benzimidazole–N-atoms reported in the equatorial plane [26]. The bond lengths Cu1–O1 2.142(5) Å and Cu1–O2 2.056(5) Å for the N-butylated complex are considerably longer than those reported in the literature for amide carbonyl coordination [27]. The bond angles in the present complexes are quite close to the values expected for an octahedral structure except the bond angles O2–Cu1–O3 163.6(2)° and O4–Cu1–O3 56.84(19)°. The distortion may be due to the combined results of Jahn teller effects and the fixed bite size of the nitrate anion. The crystal structure shows intermolecular N–H...O hydrogen bonding through amide–NH and oxygen of the lattice nitrate (Fig. 2).

The copper center in **2** is pentacoordinate consisting of two imine nitrogens of the two benzimidazole rings, two amide carbonyl oxygen atoms of the ligand and a bromide ion. The structure has the appearance of a distorted square pyramidal in which axial position is occupied by a Br atom and equatorial positions are occupied by amide carbonyl oxygen atoms O1 and O1', benzimidazole imine nitrogen atoms N2 and N2'. Cu–N bond distances of 1.966 Å for (Cu–N2 and Cu–N2') and are in the range found for similar benzimidazole and imidazole-ligated compounds [21,28,29]. Cu–O bond distances of 2.156 Å for Cu–O1 and Cu–O1' are considerably longer than those reported in the literature for amide carbonyl coordination [27] (Fig. 3).

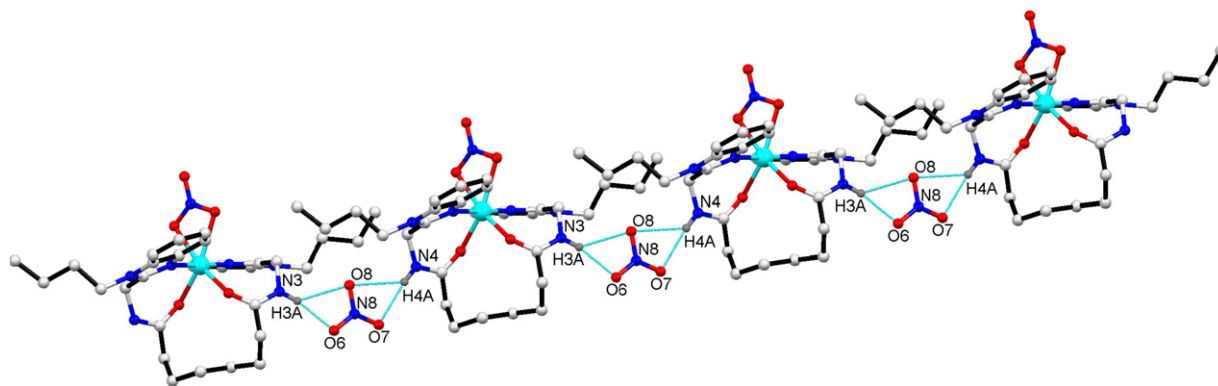


Fig. 2. The intermolecular hydrogen-bonding interactions in the crystal structure of **1**. Hydrogen atoms are omitted for clarity (red O; blue N; gray C; light blue Cu). The light green dotted bond shows the intermolecular hydrogen bonding interactions between $N3-H3A...O6 = 2.891(9)\text{\AA}$, $N3-H3A...O8 = 3.065(9)\text{\AA}$, $N4-H4A...O8 = 3.043(9)\text{\AA}$, and $N4-H4A...O7 = 2.992(8)\text{\AA}$.

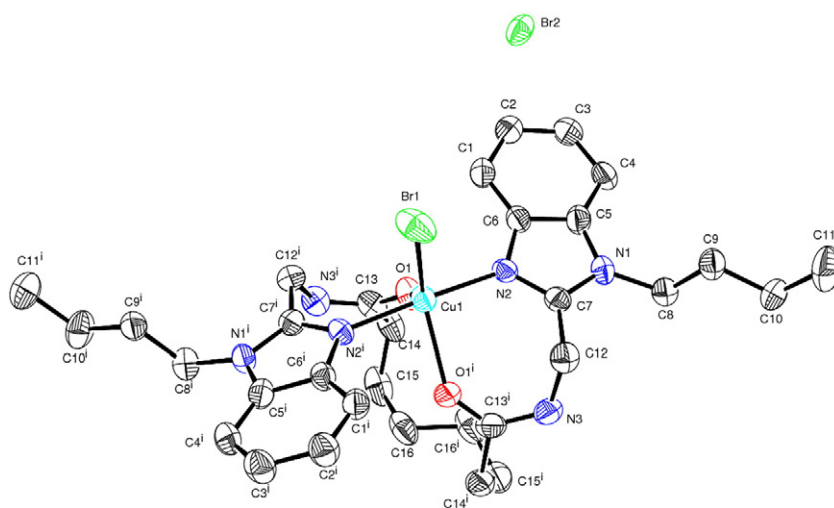


Fig. 3. Ortep diagram of compound **2** drawn in 30% thermal probability level; hydrogen atoms were omitted for clarity. Selected bond lengths (\AA) and bond angles ($^\circ$): $Cu1-Br1$ 2.3772(19), $Cu1-N2$ 1.966(5), $Cu1-N2'$ 1.967(5), $Cu1-O1'$ 2.156(5), $Cu(1)-O(1)$ 2.156(5), $N2-Cu1-N2'$ 176.3(3), $N2-Cu1-O1'$ 93.6(2), $N2'-Cu1-O1'$ 83.7(2), $N2-Cu1-O1$ 83.7(2), $N2'-Cu1-O1$ 93.6(2), $O1'-Cu1-O1$ 90.6(3), $N2-Cu1-Br1$ 91.85(16), $N2'-Cu1-Br1$ 91.85(16).

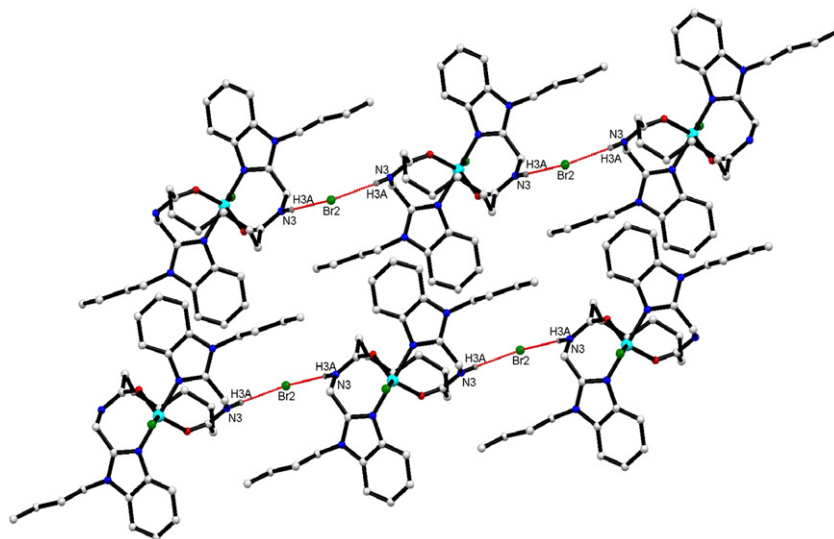


Fig. 4. The intermolecular hydrogen interactions in the crystal structure of **2**. Hydrogen atoms are omitted for clarity. Red O; blue N; white C; green Br; LIGHT Blue Cu. The dotted red line shows the intermolecular hydrogen bonding interactions between $N3-H3A...Br2 = 3.284(6)\text{\AA}$.

The uncoordinated Br anion is hydrogen bonded to the amide of the neighboring complex molecule as shown in (Fig. 4).

Our earlier work on structures of copper (II) compounds with bis-benzimidazole di-amide ligands shows the formation of mononuclear complexes when the linker spacer is four methylene carbon chain. The coordination environment around copper (II) atom is found to vary between a pentacoordinate [21] and hexacoordinate [20,30]. Some changes do occur when the benzimidazole –NH is replaced by an octyl chain which results in the conformation of the chain linking two benzimidazole rings as gaagagaag. It also results in the kink at the linker spacer C3–C4–C5–C6 giving a spiral turn to the ligand which then wraps around the metal ion in the form of half helix [20]. Further, if the benzimidazole –NH is substituted by aromatic linker like 2-picolyl resulting in a center of inversion in the crystal structure and allows the ligand to extend its arm and bind with a symmetry related copper atom, the complex forms a one dimensional polymer of the type –Cu–L–Cu–L–. In case the chain length between the benzimidazole amide groups is made smaller (from four methylene groups to three methylene groups) the result of this small chain length is lowered flexibility. This ligand then adopts an extended conformation and a di-nuclear complex results [19]. In the present case, we have increased the spacer between the benzimidazole amide groups to six methylenes, thus creating greater flexibility and substituted benzimidazole –NH with a smaller butyl chain. However, this does not lead to any major departure in the coordination geometry which

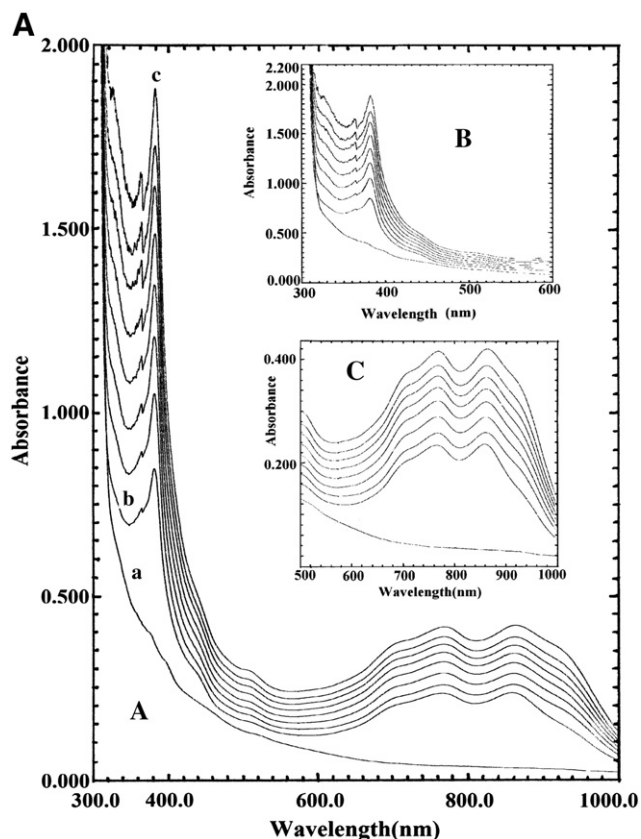


Fig. 5. (A) [Curve a] UV-visible spectra of 2-amino-4-tertiary butyl phenol (4 mM, methanolic solution). [Curve b] New peak generated in the presence of $[\text{Cu}(\text{L})\text{Cl}_2]$ (0.2 mM) solution at 2 min and [Curve c] at 80 min. Inset marked as B shows a peak at 382 nm in the region between 300 nm and 600 nm and inset marked as C shows peaks at 750 nm and 860 nm in the region of 500 nm to 1100 nm. (B) [Curve a] UV-visible spectra of 2-amino-4-tertiary butyl phenol (4 mM, methanolic solution). [Curve b] A new peak generated in the presence of $[\text{Cu}(\text{L})(\text{NO}_3)_2]$ (0.2 mM) solution at 2 min and [Curve c] at 100 min. (C) A new peak generated in the presence of $[\text{Cu}(\text{L})\text{Br}_2]$ (0.2 mM) solution with 2A4TBP [Curve a] at 2 min, [Curve b] at 58 min.

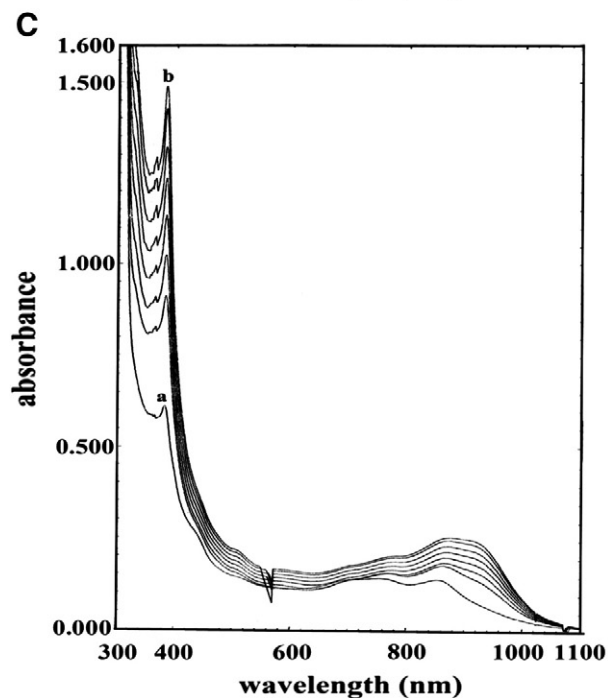
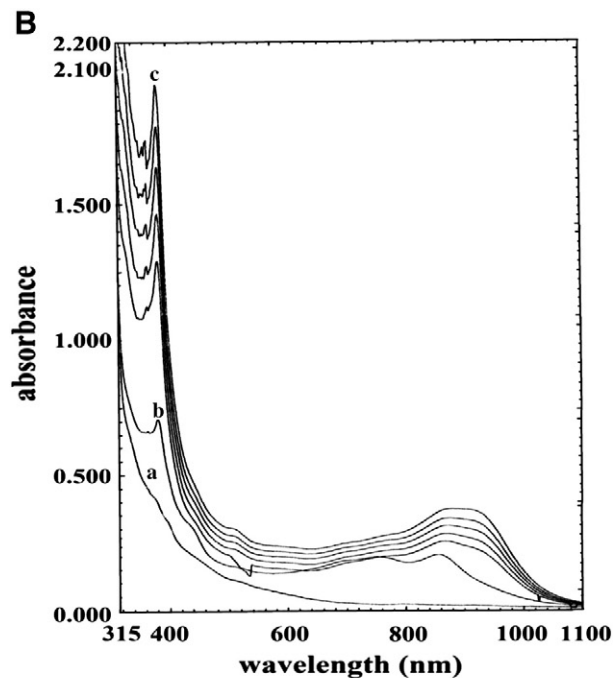


Fig. 5 (continued).

is still found to be either pentacoordinate or hexacoordinate and there is no resultant formation of 1D polymer or a dinuclear complex. However, there appears to be a change in the electrode potentials of copper (II) complexes, which in the present case with a more flexible linker are more cathodic in comparison to mononuclear copper (II) complexes where the linker chain is smaller (four methylene groups) [20,21].

The oxidation of substituted amino phenols using these copper (II) complexes was observed spectrophotometrically. A 1.0 ml (0.2 mM) methanolic solution of copper complex was added to 2.0 ml (4 mM) methanolic solution of substituted amino phenol and was placed in a 1 cm path length optical cell in a spectrophotometer. Product formation due to oxidation reaction was observed by the increase of

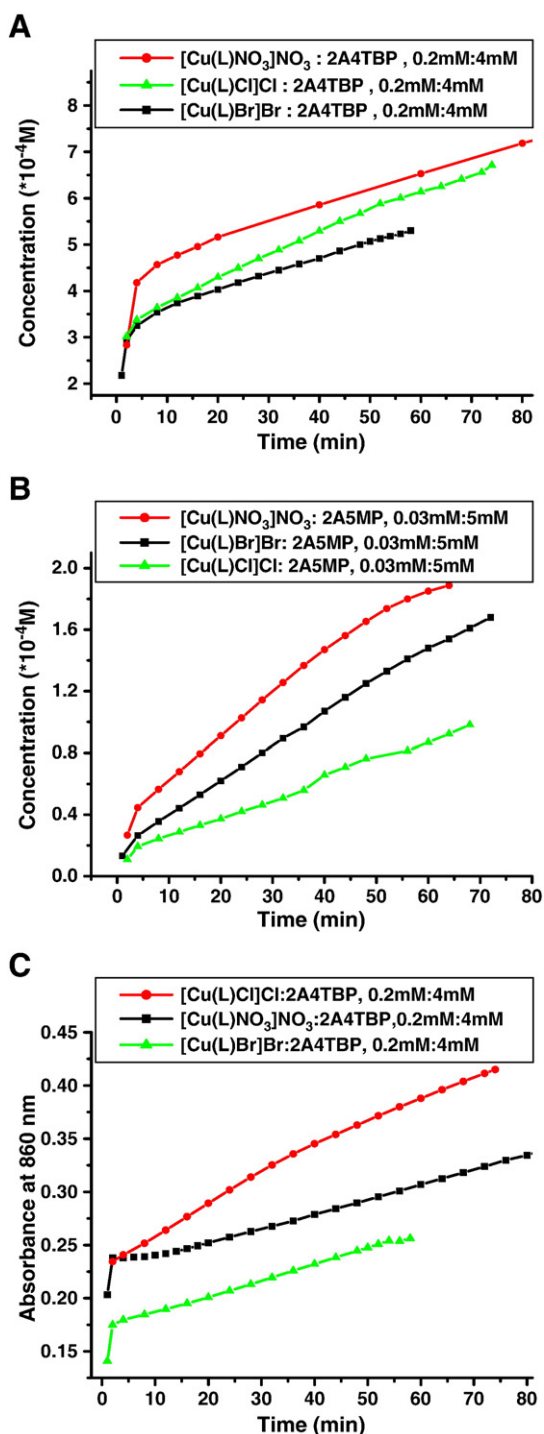


Fig. 6. Plot of concentration of product formed ($\times 10^{-4} M$) vs time (min). (A) Complex (0.2 mM): 2A4TBP (4 mM). (B) complex (0.03 mM): 2A5MP (5 mM). (C) Plot of absorbance at 860 nm vs time (min) for all the complexes (0.2 mM) with 2A4TBP (4 mM).

characteristic absorption band in the region of 380–400 nm. Blank run for substituted amino phenol was also performed in the same manner by adding 1.0 ml of oxygen saturated methanol to 2.0 ml of amino phenol solution (4 mM) in the absence of the copper complex, no new band is generated in the blank implying the role of copper (II) complexes in the oxidation reaction.

When the copper (II) complex [Cu(L)Cl]Cl is mixed with 2-amino-4-tertiary butyl phenol, new bands are generated in the region of 380 nm and 700–860 nm. The presence of a band at 380 nm suggests

the formation of o-quinone of 2-amino-4-tertiary butyl phenol [31], whereas the presence of two bands found at 760 nm and 860 nm for [Cu(L)NO₃]NO₃ suggests the formation of a new intermediate copper (II) species. This is different from the original copper (II) complexes which possess a single broad band at 760 nm. While for the [Cu(L)NO₃]NO₃ complex, new bands are generated at 380 nm, 760 nm and 860 nm. However in this case, as the reaction progresses, the band at 860 nm slowly shifts to a broad feature at 900 nm, suggesting the formation of a secondary intermediate. A similar behavior was observed for the [Cu(L)Br]Br complex. For the complex [Cu(L)Cl]Cl, the new bands associated with the intermediate species at 760 and 860 nm slowly increase in intensity as the reaction progresses and remain intact, as no shift in λ_{max} is observed for both the bands (Fig. 5A–C).

There appears to be a correlation between the average rate of reaction for the formation of the o-quinone species and the rate of formation of the intermediate copper (II) species. The average rate of reaction was obtained from the slope of the plot between concentration of the product formed and time, which gives a near linear correlation (Fig. 6A–B).

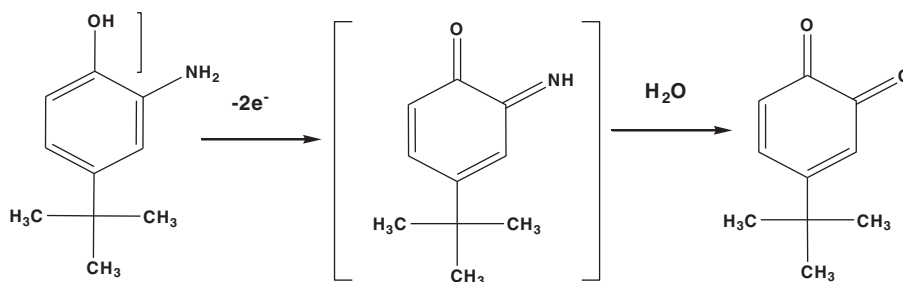
A plot of absorbance at 860 nm vs time (min) shows a steady rise for the catalyst [Cu(L)Cl]Cl, while for the corresponding [Cu(L)NO₃]NO₃, the rate of formation of the intermediate species is found to be lower than for the chloride bound complex (Fig. 6C).

This change is reflected in the average rate of the formation of the o-quinone which is found to be highest i.e. $50.0 \times 10^{-4} \text{ m ML}^{-1} \text{ min}^{-1}$ for [Cu(L)Cl]Cl complex and lower i.e. $34.0 \times 10^{-4} \text{ m ML}^{-1} \text{ min}^{-1}$ for [Cu(L)NO₃]NO₃ complex. A similar explanation can be given for the lower average rate of o-quinone formed for the [Cu(L)Br]Br complex.

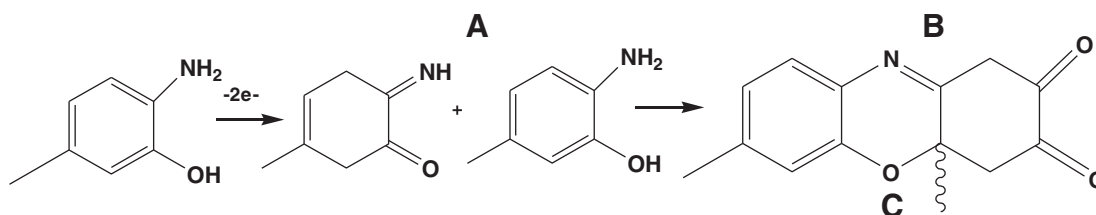
It has been reported earlier that enzyme catalyzed oxidation of 3,5-ditertiary butyl-2-aminophenol results in the formation of the intermediate o-quinoneimine, which is hydrolyzed to corresponding o-quinone rather than phenoxazinone [7]. Similarly in our case, the oxidation of 2-amino-4-tertiary butyl phenol does not result in the formation of p-quinoneimine [32]. This is confirmed from the λ_{max} of the product formed in the present case, which is found at 380 nm, rather than 566 nm as reported for p-quinoneimine. In this case, the tertiary butyl group at the 4th position blocks the conjugate addition of the second molecule of 2-amino-4-tertiary butyl phenol. Thus the product formed in the present case is o-quinone (B) generated as result of the hydrolysis of the oxidized o-quinone imine (A) (Scheme 2).

The oxidation reaction of the 2-amino-5-methyl phenol is found to be quite fast in comparison to 2-amino-4-tertiary butyl phenol (Fig. 3.1(a–c) Supplementary data). Thus in this case the concentration of the catalyst had to be lowered by 5 times so that appropriate spectral readings could be taken. Under such low concentrations, the intermediate copper (II) species that might form is not observed. In this case, the present series of copper (II) complexes catalyze the oxidation of 2-amino-5-methyl phenol to the stage of dihydrophenoxazinone (C) (Scheme 3). This is confirmed from the λ_{max} of the optical band generated during the oxidation cycle which in all cases is at around 400 nm. Had the oxidation reaction proceeded beyond the stage of dihydrophenoxazinone to phenoxazinone the λ_{max} would have shifted to 435 nm [7,32]. The average rate of reactions is $23.4 \times 10^{-4} \text{ m ML}^{-1} \text{ min}^{-1}$, $22.5 \times 10^{-4} \text{ m ML}^{-1} \text{ min}^{-1}$ and $12.4 \times 10^{-4} \text{ m ML}^{-1} \text{ min}^{-1}$ for [Cu(L)NO₃]NO₃ and [Cu(L)Br]Br and relatively lower for the [Cu(L)Cl]Cl complex respectively. The order of the average rate of reaction is different since the final product formed in this case is also different from the reaction with 2-amino-4-tertiary butyl phenol.

In summary, we find that like the enzyme catalyzed oxidation, present copper (II) complexes do not oxidize 2-amino-5-methyl phenol beyond the dihydrophenoxazinone stage and 2-amino-4-tertiary butyl phenol only to o-quinone stage (B). This is reminiscent of the functioning of the phenoxazinone synthase enzyme.



Scheme 2. Hydrolysis of intermediate orthoquinone-imine to form the final oxidized product 4-tert-butyl quinone.



Scheme 3. Condensation of intermediate orthoquinone-imine with substituted aminophenol to form the dihydrophenoxazinone.

Acknowledgment

Financial support from the University of Delhi is gratefully acknowledged. The authors also thank Mr. Kuldeep Mahiya for helping in X-ray Crystallography.

Appendix A. Supplementary material

CCDC numbers 829607 and 829608 contain the supplementary crystallographic data for **1** and **2** of this paper. These data can be obtained free of charge via www.ccdc.cam.ac.uk/conts/retrieving.html (or from the Cambridge Crystallographic Data Centre, 12, Union Road, Cambridge CB2 1EZ, UK); fax: (44) 1223-336-033; or e-mail: deposit@ccdc.com.ac.uk. Supplementary data associated with this article has also been included.

References

- [1] (a) Bioinorganic Catalysis, in: J. Reedijk, E. Bouwman (Eds.), Marcel Dekker, 1999; (b) K.D. Karlin, Z. Tyeklar, Bioinorganic Chemistry of Copper, Chapman & Hall, New York, 1993; (c) L. Casella, Eur. J. Inorg. Chem. (2006) 3545–3546; (d) J. Reedijk, Science 308 (2005) 1876–1877.
- [2] L.M. Mirica, M. Vance, D.J. Rudd, B. Hedman, K.O. Hodgson, E.I. Solomon, T.D.P. Stack, Science 308 (2005) 1890–1892.
- [3] (a) D. Maiti, A.A. Narducci Sarjeant, K.D. Karlin, J. Am. Chem. Soc. 129 (2007) 6720–6721; (b) H.C. Liang, M.J. Henson, L.Q. Hatcher, M.A. Vance, C.X. Zhang, D. Lahti, S. Kaderli, R.D. Sommer, A.L. Rheingold, A.D. Zuberbuhler, E.I. Solomon, K.D. Karlin, Inorg. Chem. 43 (2004) 4115–4117.
- [4] M.J. Colaneri, J. Peisach, J. Am. Chem. Soc. 117 (1995) 6308–6315.
- [5] E. Katz, H. Weissbach, J. Biol. Chem. 237 (1962) 882–886.
- [6] J.A. Connor, E.M. Jones, J. Chem. Soc. Dalton Trans. (1973) 2119–2124.
- [7] C.E. Barry, P.G. Nayar, T.P. Begley, J. Am. Chem. Soc. 110 (1988) 3334–3335.
- [8] Preparation of N,N'-Bis(1-butyl-benzimidazol-2-yl-methyl)-hexane-1,6-dicarboxamide (L = b-GBSA): A solution of GBSA (500 mg, 1.1567 mmol) was suspended in 20 ml of dry DMF taken in a round bottom flask (100 ml) and stirred for 4–5 h with dry K₂CO₃ (479 mg, 3.470 mmol) on a water bath at 70–75 °C temperature. When turbidity appeared n-butyl bromide (0.37 ml, 3.470 mmol) was added and the solution was left for stirring for the next 72 h on a water bath at 70–75 °C. Subsequently, the solvent was stripped off on a heating mantle and the residue was extracted with chloroform (insoluble part was rejected). Upon adding hexane to this filtrate, a white precipitate was deposited, which was washed with hexane, dried and recrystallized using methanol. The product was filtered off and dried. Yield: (300 mg) 60%. ¹H NMR (400 MHz, CDCl₃): δ(ppm) = 9.83–9.86 (2H, t), 7.61–7.64 (4H, m), 7.22–7.35 (4H, m), 4.64–4.65 (4H, d), 2.38–2.41 (4H, t), 1.75–1.82 (4H, m), 1.66 (br,4H, m), 4.22–4.26 (4H, t), 1.34–1.43 (br,4H), 1.21 (br, m, 4H), 0.92–0.96 (6H, t); ¹³C NMR (d⁶-DMSO): (C4, C7) 118, (C8, C9) 135, (C5, C6) 122, (C2) 152, e 32, C=O 32, C 36, b 25, a 28, i 43, j 32, K 19, L 13; Anal Calcd for C₃₂H₄₄N₆O₂: C 70.5, H 8.0, N 15.4, Found: C 69.1, H 7.5, N 15.3. λ_{max} (nm) [log ε] in DMF = 281[4.81], 274 [4.83].
- [9] Synthesis of complexes (**1**), (**2**), and (**3**): A solution of [Cu(NO₃)₂·3H₂O, CuBr₂ and CuCl₂·2H₂O] (1 mmol) in 5 ml of methanol was added to a solution of L (1 mmol) in 5 ml of methanol. The mixture was stirred for 3–4 h. The precipitated green products were filtered off, washed with small amounts of acetonitrile and dried over P₂O₅. Suitable single green crystals for **1** and **2** were obtained on slow evaporation. **1**: Yield: (73%). C₃₂H₄₄CuN₆O₈ (732.29): Calcd (%) C 52.5, H 6.0, N 15.3; Found C 51.3, H 6.8, N 14.6; IR (KBr, cm⁻¹): 3235(ν_{NH} amide I), 1617 (ν_{C=O} amide I), 1560 (ν_{C-N} amide II); UV (DMF): λ_{max} (nm) (log ε): 273(3.95), 281(3.90), 743(1.83). **2**: Yield: (70%). C₃₂H₄₄Br₂CuN₆O₂ (768.09): Calcd (%) C 47.3, H 6.0, N 10.3; found C 46.5, H 5.7, N 9.6; IR (KBr, cm⁻¹): 3280(ν_{NH} amide), 1618(ν_{C=O} amide I), 1542 (ν_{C-N} amide II); UV (DMF) λ_{max} (nm) (log ε): 277(4.12), 287(4.05), 747(2.38). **3**: Yield: (68%). C₃₂H₄₄Cl₂CuN₆O₂ (714.5): Calcd (%) C 53.7, H 6.7, N 11.7; found C 53.3, H 7.3, N 11.6; IR (KBr, cm⁻¹): 3231(ν_{NH} amide), 1618 (ν_{C=O} amide I), 1560 (ν_{C-N} amide II); UV (DMF): λ_{max} (nm) (log ε): 274(4.55), 281(4.49), 750(2.20).
- [10] Single crystals suitable for X-ray diffraction studies were grown by slow evaporation in methanol. The intensity data were collected at 295 K on Xcalibur CCD diffractometer with graphite monochromatized Mo Kα radiation. The intensity data were corrected for Lorentz and polarization effects. No absorption correction was applied. The structure was solved by direct methods using SIR-92 [11] and refined by full-matrix least-squares refinement techniques on F², using SHELXL-97 [12]. All calculations were done with the help of WINGX programme [13]. The weighted R factor, wR₂ and goodness of fit S are based on F², the conventional R factor is based on F with F set to zero for negative F². All non-hydrogen atoms were refined anisotropically. Hydrogens of the water molecule were located from the difference Fourier and were refined isotropically initially for a few cycles. Crystal data for compound **1**: C₃₂H₄₄CuN₆O₈, M_r = 732.29 T = 120(2) K, triclinic, P-1, a = 11.9194(17) Å, b = 11.9616(17) Å, c = 12.2773(11) Å, α = 86.360(10)°, β = 83.617(10)°, γ = 89.869(12)°, V = 1736.1(4) Å³, Z = 2, d = 1.401 mg/m³, F(000) = 770, 0.20 × 0.14 × 0.10 mm³, 2θ = 26.00°, -14 ≤ h ≤ 14, -10 ≤ k ≤ 14, -15 ≤ l ≤ 14, 13,102 reflections were collected and 6690 are unique, R_{int} = 0.0515, GOF = 1.080, R₁ = 0.0946, WR₂ = 0.2593. Crystal data for compound **2**: C₃₂H₄₄Br₂CuN₆O₂, M_r = 768.09, T = 298(2) K, monoclinic, C2/c, a = 17.881(2) Å, b = 16.5552(17) Å, c = 11.8886(12) Å, α = 90°, β = 101.04(11)°, γ = 90°, V = 3454.1(6) Å³, Z = 4, d = 1.477 mg/m³, F(000) = 1572, 0.22 × 0.20 × 0.16 mm³, 2θ = 68.00°, -21 ≤ h ≤ 21, -19 ≤ k ≤ 19, -11 ≤ l ≤ 14, 6492 reflections were collected and 2989 are unique, R_{int} = 0.0788, GOF = 0.905, R₁ = 0.0604, WR₂ = 0.1040.
- [11] A. Altomare, M.C. Burla, M. Camalli, G. Casciarano, C. Giacovazzo, A. Guagliardi, A.G.G. Moliterni, G. Polidori, R. Spagna, SIR-92, A New Programme for Solving and Refining Structures, 1997.
- [12] G.M. Sheldrick, SHELXL-97, Programme for Crystal Structure Refinement, University of Göttingen, Germany, 1997.
- [13] L.J. Farugia, WINGX, an integrated system of Windows programs for the solution, Refinement and Analysis of Single Crystal X-ray Diffraction Data, University of Glasgow, Glasgow, 2006.
- [14] L.A. Cescon, A.R. Day, J. Org. Chem. 27 (1962) 581–586.
- [15] R. Bakshi, P. Mathur, Inorg. Chim. Acta 363 (2010) 3477–3488.
- [16] F. Afreen, P. Mathur, A. Rheingold, Inorg. Chim. Acta 358 (2005) 1125–1134.

- [17] M. Gupta, S.K. Das, P. Mathur, A.W. Cordes, *Inorg. Chim. Acta* 353 (2003) 197–205.
- [18] S.K. Upadhyay, S. Tehlan, P. Mathur, *Spectrochim. Acta, Part A* 66 (2007) 347–352.
- [19] S.C. Mohapatra, S. Tehlan, M.S. Hundal, P. Mathur, *Inorg. Chim. Acta* 361 (2008) 1897–1907.
- [20] S. Menage, L. Que Jr., *Inorg. Chem.* 29 (1990) 4293–4297;
b) S. Tehlan, M.S. Hundal, P. Mathur, *Inorg. Chem.* 43 (2004) 6589–6595.
- [21] M. Gupta, P. Mathur, R.J. Butcher, *Inorg. Chem.* 40 (2001) 878–885.
- [22] W.J. Geary, *Coord. Chem. Rev.* 7 (1971) 81–122.
- [23] G. Batra, P. Mathur, *Inorg. Chem.* 31 (1992) 1575–1580.
- [24] Rajesh, P. Mathur, *Polyhedron* 17 (1998) 2607–2615.
- [25] H.M.J. Hendriks, P.J.M.W.L. Birker, J.V. Rijn, G.C. Verschoor, J. Reedijk, *J. Am. Chem. Soc.* 104 (1982) 3607–3617.
- [26] M. Gupta, S.K. Upadhyay, M.A. Sridhar, P. Mathur, *Inorg. Chim. Acta* 359 (2006) 4360–4366.
- [27] (a) H.J. Prochaska, W.F. Shwindinger, M. Schwartz, M.J. Burk, E. Bernarducci, R.A. Lalancette, J.A. Potenza, H.J. Schugar, *J. Am. Chem. Soc.* 103 (1981) 3446–3455;
(b) V. Jeffery, V.M. Dagdigian, C.A. Reed, *Inorg. Chem.* 21 (1982) 1332–1342.
- [28] N.R. Sangeetha, K. Baradi, R. Gupta, C.K. Pal, V. Manivannan, S. Pal, *Polyhedron* 18 (1999) 1425–1429.
- [29] (a) S.S. Tandon, L.K. Thompson, J.N. Bridson, J.C. Dewan, *Inorg. Chem.* 33 (1994) 54–61;
(b) A.W. Addison, P.J. Burke, K. Henrick, T.N. Rao, E. Sinn, *Inorg. Chem.* 22 (1983) 3645–3653;
(c) E. Monzani, L. Quinti, A. Perotti, L. Casella, M. Gulloti, L. Randaccio, S. Geremia, G. Nardin, P. Faleschini, G. Tabbi, *Inorg. Chem.* 37 (1998) 553–562.
- [30] R. Bakshi, M. Rossi, F. Caruso, P. Mathur, *Inorg. Chim. Acta* 376 (2011) 175–188.
- [31] S.P. Harmalker, D.T. Sawyer, *J. Org. Chem.* 49 (1984) 3579–3583.
- [32] M. Giurg, K. Piekielska, M.G. bala, B. Ditkowski, M. Wolanski, W.P. Czoch, J. Mlochowski, *Synth. Commun.* 37 (2007) 1779–1789.